TSG-RAN WG4 Meeting #69 **R4- 135809**
San Francisco, USA, November 11th – 16rd, 2013

Title:	AAS radiated performance comparison between MIMO MOTA test methodologies
Source:	Motorola Mobility LLC, Intel, Aalborg University
Agenda Item:	8.3
Work Item:	HSPA_LTE_measRP_MIMO-Perf
Release:	12
Document for:	Discussion

1. Abstract

This contribution describes the radiated performance of an active antenna system (AAS) UE test fixture, featuring a tunable antenna with four states, performs analysis of absolute data throughput, comparing results between anechoic chamber boundary array and reverberation chamber.

2. Introduction

In the scope of the work done in 3GPP RAN4 on MIMO OTA, a number of companies have raised the question of the ability of test methodologies to discriminate various antenna designs. The CTIA reference antennas [1] have provided a baseline for the work in 3GPP and CTIA to advance but do not cover the vast and diverse number of antenna design techniques utilized in the industry to improve channel capacity and ultimately throughput. In [2] and [3] it was clearly shown that reverberation chamber based methodologies are incapable of distinguishing antenna designs with pure polarization diversity. A Device Under Test (DUT) utilizing polarization diversity would then be seen only through its antenna efficiency and the only benefit of the utilization of polarization diversity on the DUT would be potentially lower correlation between antennas. This however does not allow for antenna designers to optimize for power collection from realistic environments since any such optimization will not be seen in a reverberation chamber as shown in [2] and [3]. This is due to the fundamental limitation of the reverberation chamber to produce any other propagation conditions but those with environment XPR = 0, at least not as promoted and used to date. It must be noted here that environment XPR reported in the peer reviewed literature varies significantly and the propagation and antenna experts from COST IC1004 summarized a strong technical objection to and environment with XPR = 0 in [4].

Another aspect of antenna design not addressed with the CTIA reference antennas from [1] is the actively tunable and Adaptive Antenna System (AAS). AASs come in various flavors with many different techniques to tune impedance, pattern, polarization etc. and of course any combination of those together. Every tuning component comes at a dollar cost but also at the expense of total antenna efficiency since the tunable components are typically utilized after the calibrated RF connector. It is very important that antenna design freedom and innovation is not stifled by the evaluation methodology's incapability to demonstrate the benefits of a particular innovation. While a reverberation chamber would probably demonstrate 0.5 dB lost in total antenna efficiency due to an antenna tuner for example, the benefit from that tuner in a realistic propagation environment with non-zero XPR or directive incoming power might be completely ignored. Again the propagation and antenna experts from COST IC 1004 sound the alarm in [4]. To put this argument into perspective consider the case of beam forming and a very small sample of a vast pool of peer reviewed literature dealing with this issue.

3. Antenna Design

The sections below describe a simple beam forming design. We have not optimized for efficiency or produced an antenna ready for integration in real devices but simply continued on the original CTIA reference antenna track of demonstrating antennas principles.

3.1 Main Antenna

The main antenna is shown in Fig. 3.1-1 extends few millimeters out of the PCB. The main antenna is passive broadband top loaded monopole. It covers both TX and RX of the European LTE Band 7. The center RX frequency is 2655 MHz and the center TX frequency is 2535 MHz.

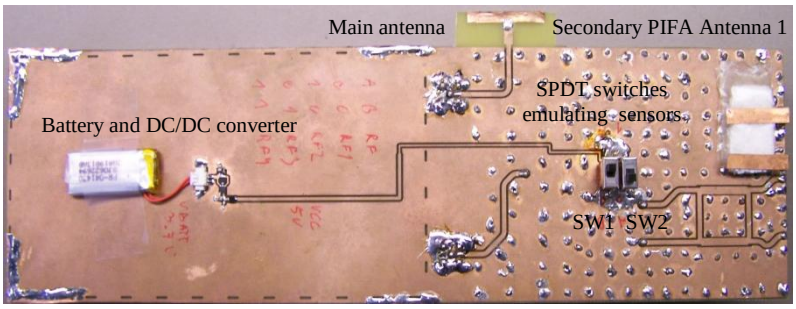

(a)

(b)

Fig. 3.1-1, AAS prototype back view (a), front view (b)

3.2 AAS for Diversity

The diversity antenna covers only the RX LTE Band 7 with a center frequency of 2655 MHz. It consists of four PIFA elements – two on the front and 2 on the back of the platform PCB – see Fig. 3.1-1 (a,b). The elements are fed via two 3dB, 90 degrees couplers implemented as microstrip lines on the PCB as shown in Fig. 3.1-1(a,b).

The front two elements shown in Fig. 3.1-1 (b) top left corner form a beam forming pair combined at the coupler. The same is done for the back two elements combined at the second coupler. The front pair covers roughly the front hemisphere of the spherical coordinate system and the back pair covers the other hemisphere. By selectively feeding the couplers' ports the beam can be steered not only between hemispheres but within a single quadrant of one hemisphere.

3.3 RF Switching and power supply

The RF switching is done with an internally terminated RF switch from Hittite Microwave Corporation [5]. The switch requires a power supply and control bits for the four different states. This is done using a DC-DC converter based on a single chip solution from Texas Instruments [6]. The battery supply is delivered from a small single Li-Io cell. The circuit is placed on the back side of the RF enclose.

The RF switch circuit is shown in Fig. 3.1-1. The two SPDT switches SW1 and SW2 are uses manually to operate the beam direction by switching the main RF switch between the four states. Clearly on a real product all of this would be optimized for performance, power consumption, sensor array and smart algorithm would control the switching.

The truth table for U2 can be found in [7]. The same RF port notation is used here.

4. Measurement Results

4.1 Antenna FoM measurement results

The Table 4.1-1 summarizes the antenna FoM measurement results, antenna 1 called “secondary” is the one being adapted, and antenna 2 is the main antenna.

Table 4.1-1 MIMO B7 antennas FoM based on 3D isotropic measurements @ 2655MHz

MIMO B7 antennas FoM based on 3D isotropic measurments @ 2655MHz					
tuner position	ant. position	Total Efficiency (%)	Polarization Ratio V/H (dB)	Branch imbalance (dB)	*ρe*
00	Antenna 1 (secondary)	41.10	0.00	3.016	0.0014
	Antenna 2 (Main)	82.30	0.70		
01	Antenna 1 (secondary)	35.10	0.30	3.717	0.0124
	Antenna 2 (Main)	82.60	0.80		
11	Antenna 1 (secondary)	35.80	0.50	3.551	0.0186
	Antenna 2 (Main)	81.10	0.70		
10	Antenna 1 (secondary)	43.40	0.60	2.774	0.0125
	Antenna 2 (Main)	82.20	0.80		

As indicated in Table 4.1-1, the antenna system has polarization ration near 0 dB, which is characteristic to antennas at high frequencies in small form factors. The envelope correlation is smaller than 0.1 guaranteeing uncorrelated antennas; at least at uniform incoming power; however the branch imbalance is near 3dB.

The following Figs. 4.1-1~7, shows the antennas return loss and radiation patterns in 3D and polar format, in different tuner positions. As indicated in Table 1, the main antenna maintains the same total efficiency and radiation patterns across all four tuner positions. The difference in performance < 0.1dB, is within the anechoic chamber measurement uncertainty.

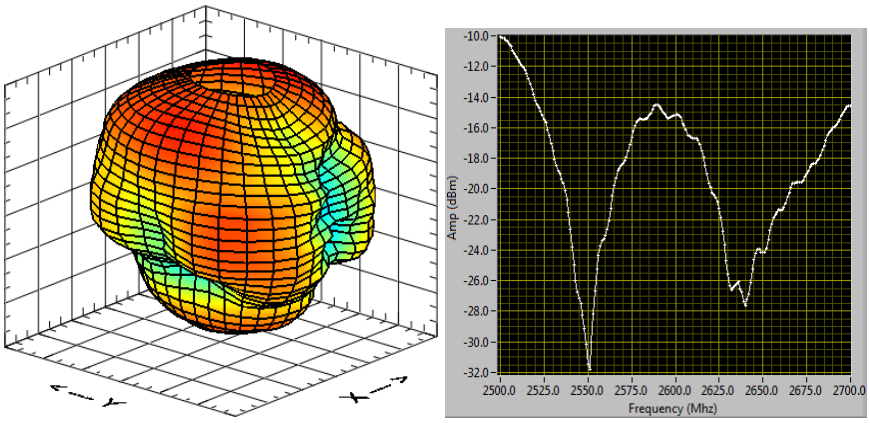

Fig. 4.1-1, Main antenna 3D free space radiation pattern, and return loss.

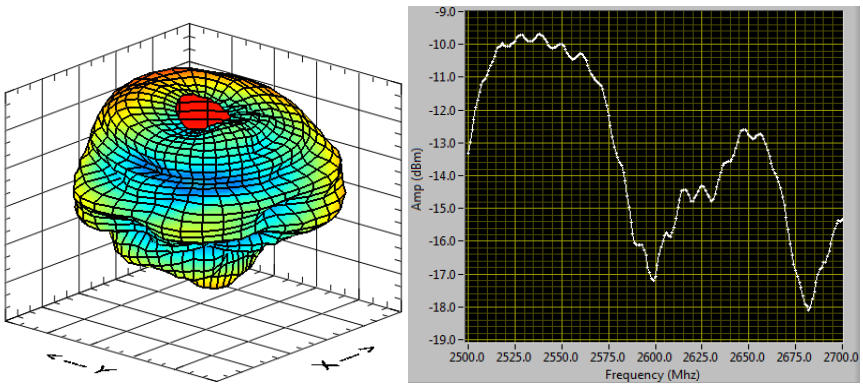

Fig. 4.1-2, Secondary antenna 3D radiation pattern, and return loss at tuner position 00.

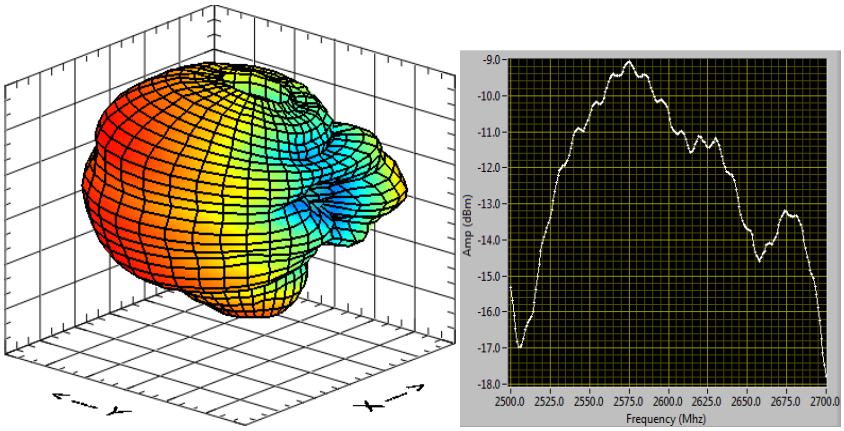

Fig. 4.1-3, Secondary antenna 3D radiation pattern, and return loss at tuner position 01.

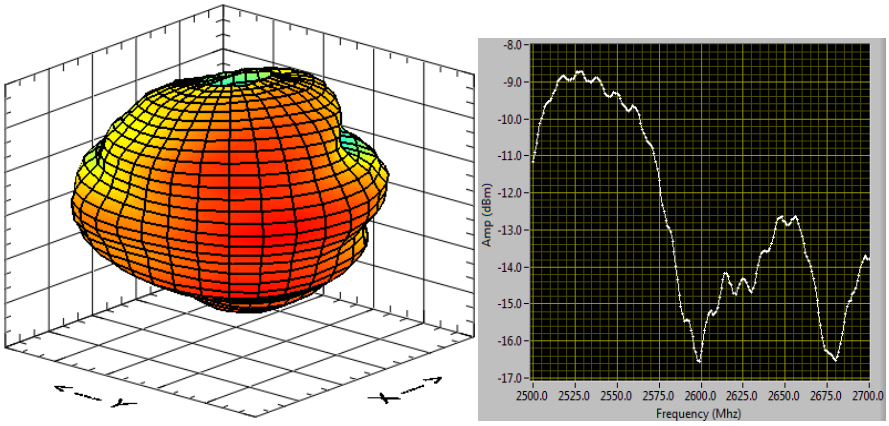

Fig. 4.1-4, Secondary antenna 3D radiation pattern, and return loss at tuner position 11.

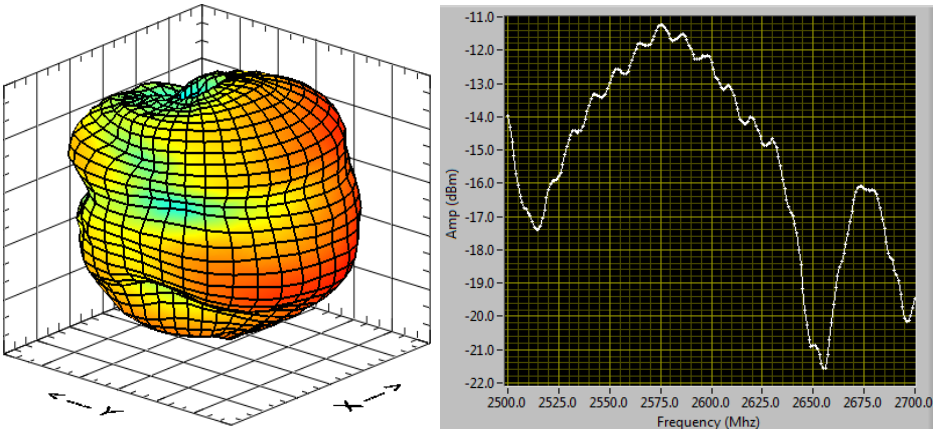

Fig. 4.1-5, Secondary antenna 3D radiation pattern, and return loss at tuner position 10.

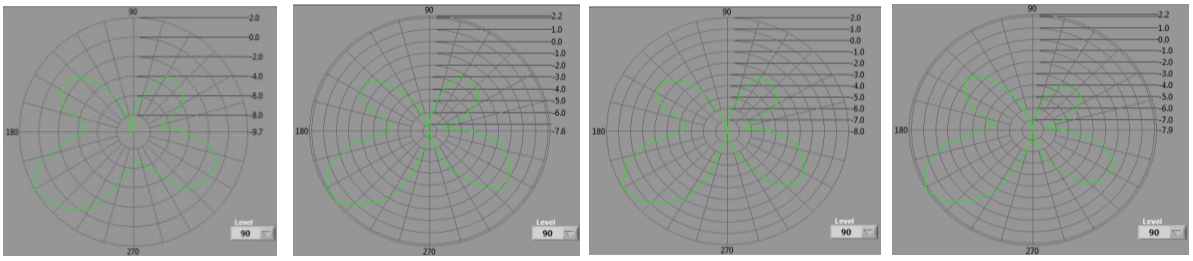

(a) (b) (c) (d)

Fig. 4.1-6, Main antenna polar plot at elevation 90°, (a) tuner position 00, (b) 01, (c) 11, (d) 10

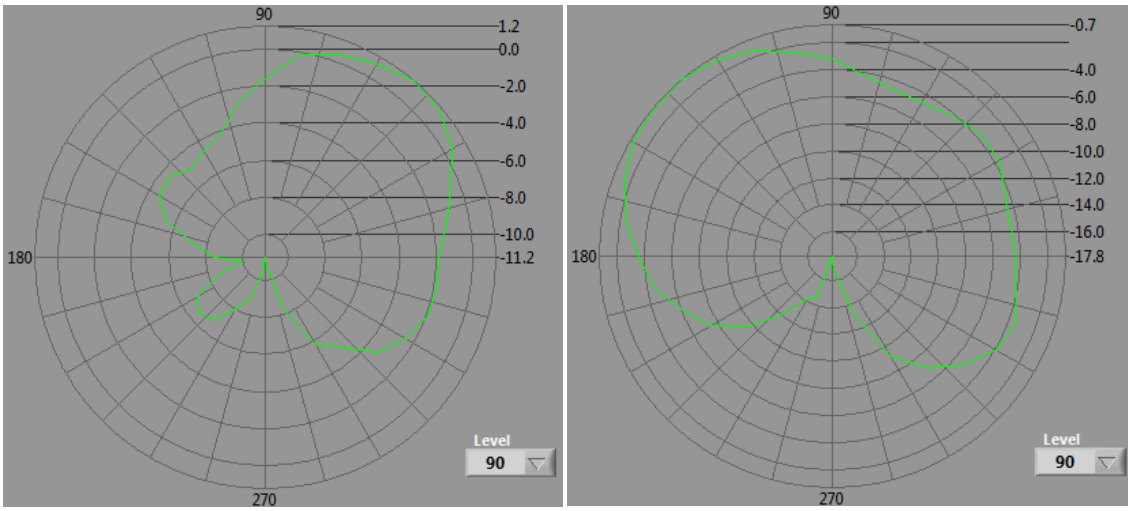

(a)

(b)

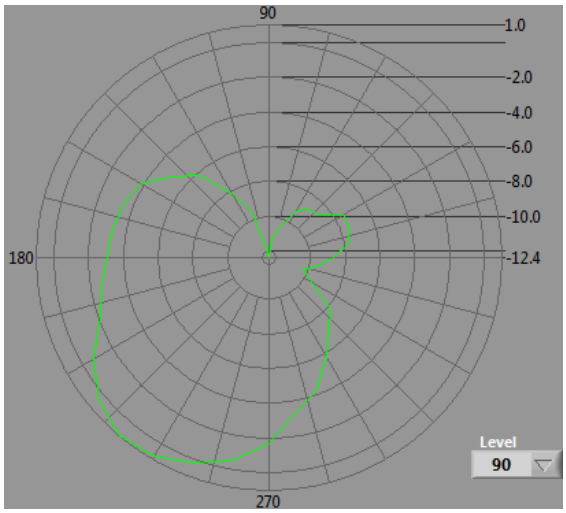

(c)

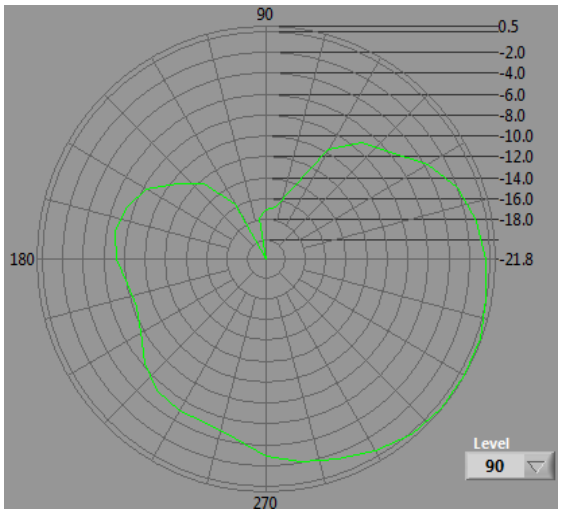

(d)

Fig. 4.1-7, Secondary antenna polar plot at elevation 90°, (a) tuner position 00, (b) 01, (c) 11, (d) 10

4.2 MIMO OTA absolute data throughput measurement results

The OTA measurement results are based in two test methodologies considered valid, the anechoic chamber multi-cluster boundary array, and the reverberation chamber without channel emulation assistance. As indicated in the Table 4.1-1, there is a branch imbalance between antennas averaging 3.3 dB, during these measurements a 3 dB series attenuator was placed between the main antenna and the DUT RF port. Thus equalizing both antennas gain. Note that this specifically DUT has additional 0.7 dB insertion loss in the secondary antenna RF port to the respective receiver, however not account for in these data results.

4.2.1 Anechoic chamber setup.

The OTA test system consisted of an ETS-Lindgren AMS-8700 boundary array with eight active dual polarized antennas at a radius of 1.95 meters driven by two Spirent VR5 8 output channel emulators for 16 total output channels used to generate the applied channel model and resulting signal levels within the test volume. Two ETS-Lindgren 8-channel power amplifiers were used to amplify the outputs of the channel emulators to produce the required signal levels within the test volume. The reported measurements were captured using a Rohde & Schwarz CMW-500 as the eNodeB emulator/communication tester. The two outputs were each split and fed into the two VR5s. A separate circularly polarized conical log spiral antenna was used to provide the uplinik from the DUT. The uplink path was then fed through a pre-amplifier to provide additional downlink isolation prior to feeding the signal to the eNodeB input. The Fig. 4.2.1-1 contains a system schematic for the test setup, while Table 4.0.1-1 contains the detailed equipment list.

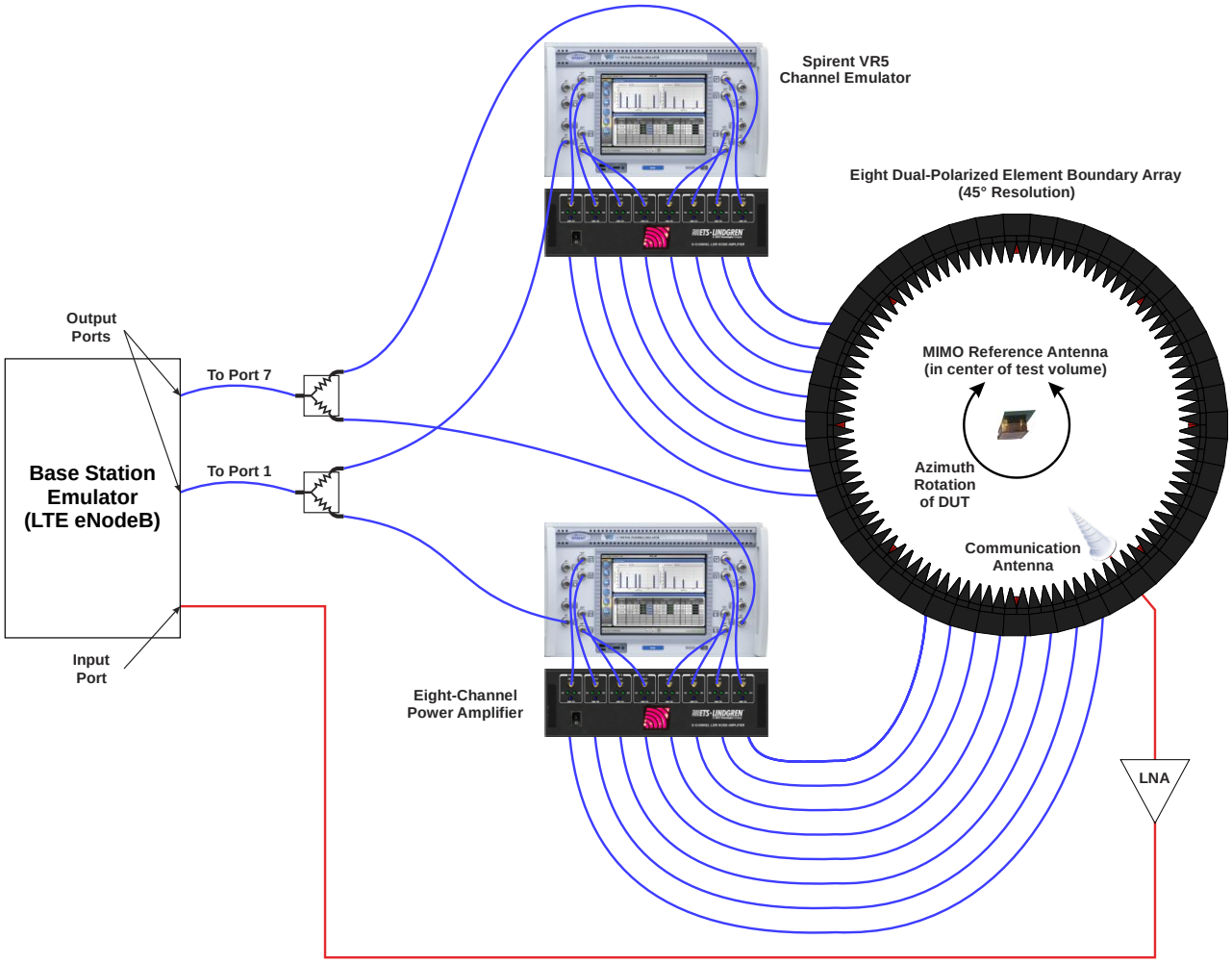

Fig 4.2.1-1 ETS-Lindgren AMS-8700 Boundary Array Schematic Diagram

Table 4.0.1-1, Anechoic chamber test equipment list

Equipment	Manufacturer	Model	Firmware Revision
MIMO Boundary Array System	ETS-Lindgren	AMS-8700	NA
Channel Emulator (2X)	Spirent	VR5	2.5.341.3
8-Channel Power Amplifier (2X)	ETS-Lindgren	P/N 117907	NA
eNodeB Emulator/ Communication Tester	R&S	CMW-500	3.2.20
Power Splitters (2X)	Mini Circuits	ZFSC-2-2500-S+	NA
Uplink Preamp	ETS-Lindgren	NA	NA

4.2.2 Reverberation chamber setup

An ETS-Lindgren AMS-7000 wireless OTA reverb test system was used to perform the average isotropic (uniform probability distribution) testing. The system consists of a compact reverberation chamber (2.00 x 1.20 x 1.50 m) with two independent stirring paddles and a DUT turntable having a lowest operating frequency of ~700 MHz, connected to a Rohde & Schwarz CMW-500 as the eNodeB emulator/communication tester. The cell was selectively loaded to produce an RMS delay spread of 80 ns for the NIST model. Tests were performed using continuous stirring of all positioners for an integral number of rotations of all positioners at a fixed ratio and timed such that one long throughput measurement was performed per revolution of the slowest positioner, thus producing one average throughput measurement per power level.

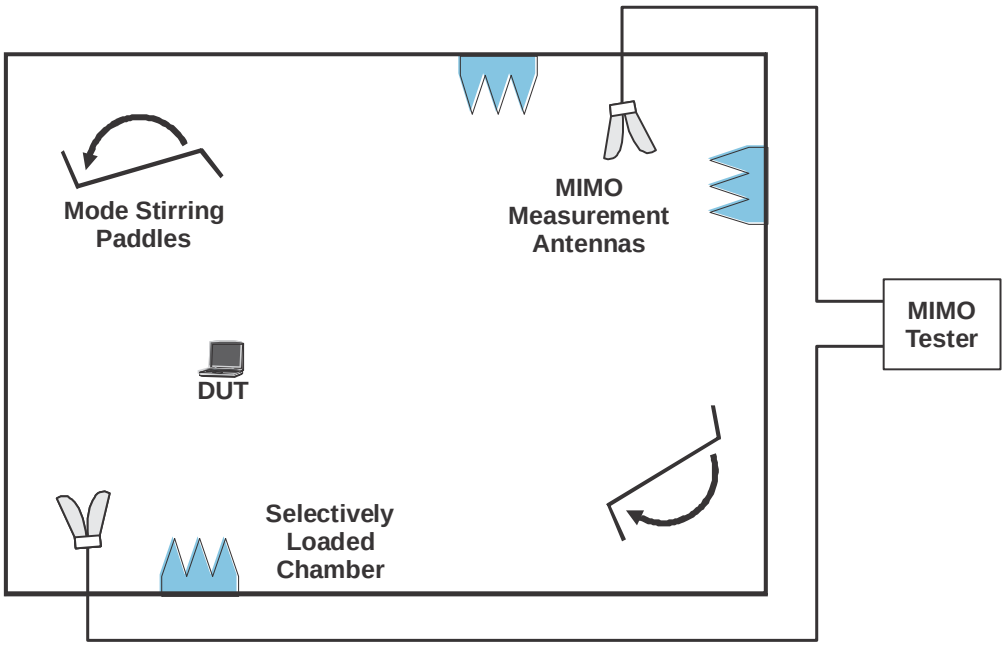

Fig 4.2.2-1, ETS-Lindgren Reverberation chamber schematic diagram

4.3 Absolute data throughput, equipment settings

The table 4.3-1 bellow presents the complete list of equipment settings used during these measurements. Allowing any lab to reproduce the data presented in this work.

Table 4.3-1 Anechoic and reverberation chamber test setup settings

Test settings	Anechoic chamber settings	Reverberation chamber settings
ID	AC AAS v1	RC AAS v1
Lab	ETS-Lindgren – Cedar Park	ETS-Lindgren – Cedar Park
Date	11/05/2013	11/05/2013
Methodology	Anechoic chamber Multi-cluster, 8DP	Reverberation chamber
eNodeB emul.	R&S CMW500	R&S CMW500
eNodeB emul. ver	Installed SW V 3.2.20	Installed SW V 3.2.20
eNodeB ant config	Sec 7.2 in 37.977	Sec 7.2 in 37.977
eNodeB PHY config	Sec 7.1 in 37.977	Sec 7.1 in 37.977
Band	7	7
DL channel	5230	5230
UL channel	23230	23230
RMC	R35	R35
Num subframes per SNR pt	5000	5000
Channel emul.	Spirent VR5	NA
Channel emul. ver	2.5.341.3	NA
Channel model config	Sec 8.2 in 37.977	NA
Channel model	SCME Umi	NIST, 80 ns delay spread
Emul. veh. speed	30 km/h	NA
UE mfg	Motorola	Motorola
UE model	XT1052	XT1052
UE ID	IMEI: LXRR2290036	IMEI: LXRR2290036
Transmission Mode	TM3	TM3
Max theoretical throughput	35.424 Mb/s	35.424 Mb/s
Num theta pos.	Sec 9.3.1.3 in 37.977	NA
Theta pos.	Sec 9.3.1.3 in 37.977	NA
Num phi pos.	Sec 9.3.1.3 in 37.977	NA
Phi pos.	Sec 9.3.1.3 in 37.977	NA
Test plan version	Lab “E1” 001	Lab “E2” 001
Comments	XPR = 9dB , 3dB attenuation in main antenna	3dB attenuation in main antenna

5 Future work (in progress)

5.1 Anechoic chamber multi-cluster boundary array absolute data throughput results

The measurements defined in “a ~ d”, will indicate the absolute data throughput results with the DUT at each tuning state. The measurement defined in “e” is a compilation of the previous measurements indicating the DUT performance as the AAS was implemented.

a. Absolute data throughput, 12 DUT rotations individual curves, and average of 12 individual curves. SCME Umi, 30kph, XPR=9dB, tuner position 00.

b. Absolute data throughput, 12 DUT rotations individual curves, and average of 12 individual curves. SCME Umi, 30kph, XPR=9dB, tuner position 01.

c. Absolute data throughput, 12 DUT rotations individual curves, and average of 12 individual curves. SCME Umi, 30kph, XPR=9dB, tuner position 11.

d. Absolute data throughput, 12 DUT rotations individual curves, and average of 12 individual curves. SCME Umi, 30kph, XPR=9dB, tuner position 10.

e. Absolute data throughput, optimal selection of 12 DUT rotations individual curves, and average of 12 optimal individual curves. SCME Umi, 30kph, XPR=9dB, AAS virtually implemented.

5.2 Reverberation chamber absolute data throughput results

The measurements defined in “a ~ d”, will indicate the absolute data throughput results with the DUT at each tuning state.

a. Absolute data throughput, NIST (80ηs RMS Delay Spread) Isotropic channel model, tuner position 00.

b. Absolute data throughput, NIST (80ηs RMS Delay Spread) Isotropic channel model, tuner position 01.

c. Absolute data throughput, NIST (80ηs RMS Delay Spread) Isotropic channel model, tuner position 11.

d. Absolute data throughput, NIST (80ηs RMS Delay Spread) Isotropic channel model, tuner position 10.

Conclusions

In this paper a simplified however realistic implementation of AAS in B7 was presented. While the sensor and action taking functions are not part of this prototype implementation, the antenna pattern rotation implementation is feasible of be implemented in commercial devices. From this experiment some preliminary conclusions can be drawn.

- The AAS antenna prototype radiation pattern measurements agree with design proposal and simulation results;

The absolute data throughput measurement results defined in section 5, are in progress and couldn't be concluded within this submission deadline. These results and respective conclusions will be resubmitted as a revision of this contribution.

References

[1] I. Szini, G. F. Pedersen, J. Estrada, A. Scannavini, and L. J. Foged, "Design and verification of MIMO 2x2 reference antennas," in *Antennas and Propagation Society International Symposium (APSURSI), 2012 IEEE*, 2012, pp. 1–2.

[2] Motorola Mobility LLC, ETS-Lindgren, Spirent Communications, "R4-134154- DUT Polarization discrimination, among MIMO OTA test methods," presented at the R4-68, Barcelona, 2013.

[3] Motorola Mobility LLC, "R4-135424 - Update results on DUT Polarization discrimination among MIMO OTA test," presented at the R4-68_bis, Riga, Latvia, 2013.

[4] Aalborg University, Motorola Mobility LLC, Anite Telecoms ltd, "R4-135433 - COST IC1004 TWGO comments on proposal for additional channel models for MIMO OTA performance," presented at the R4-68_bis, Riga, Latvia, 2013.

[5] Hittite Microwave Corporation, "HMC241LP3 / HMC241LP3E - SP4T Non-Reflective Switch SMT, DC - 4 GHz." Hittite Microwave Corporation.

[6] Texas Instruments, "TPS61240 - 5V, 400mA, 4MHz Step-Up DC/DC Converter." Texas Instruments.

[7] Intel Corporation, Motorola Mobility LLC, Aalborg University, "R4-136185 - MIMO AAS spatially filtered channel model simulations," presented at the R4-69, San Francisco, USA, 2013.